Formation of quasistationary vortex and transient hole patterns through vortex merger

R. Ganesh[a] and J. K. Lee[b]
Department of Electrical Engineering, Pohang University of Science and Technology (POSTECH), Pohang 790-784, South Korea

(Received 1 July 2002; accepted 26 July 2002)

Collection of point-like intense vortices arranged symmetrically outside of a uniform circular vortex patch, both enclosed in a free-slip circular boundary, are numerically time evolved for up to 10–15 patch turnover times. These patterns are found to merge with the patch by successively *inducing* nonlinear dispersive modes (*V*-states) on the surface of the patch, draw off fingers of vorticity (filamentation), trap the irrotational regions as the fingers symmetrize under the shear flow of the patch and point-like vortices (wave breaking) followed by the vortex–hole capture. While the hole patterns are observed to break up over several turnover periods the vortex patterns appear to evolve into quasistationary patterns for some cases of an initial number of point-like vortices N_{pv}. The bounded *V*-states, filamentation, and vortex (hole) pattern formation are discussed in some detail and their possible connection to recently observed vortex ''crystals'' is pointed out.
 [DOI: 10.1063/1.1513154]

I. INTRODUCTION

Both in experiments and numerical simulations, intense vortices have been observed to form in decaying inviscid, incompressible, two-dimensional (2D) turbulence.[1,2] The interaction between these strong vortices and holes (regions of zero vorticity) with the background turbulence is believed to play a crucial role in determining the eventual state of turbulence. Consequently, the study of coherent structures (vortices/holes) in a background flow in the context of 2D turbulence has gained tremendous attention.

Incompressible, inviscid, 2D turbulence and magnetized plasma columns under conditions of strong axial magnetic field $B\,\hat{z}$ and low dissipation[3] are known to be governed by the same equations viz.,

$$(\partial_t + \mathbf{v}\cdot\boldsymbol{\nabla})n = 0, \tag{1}$$

where the drift velocity $\mathbf{v}=\mathbf{v}(r,\theta,t)$ related to the electrostatic potential $\varphi=\varphi(r,\theta,t)$ is given by

$$\mathbf{v} = \hat{z}\times\nabla\varphi/B \tag{2}$$

and density $n=n(r,\theta,t)$ satisfies the Poisson's equation,

$$\nabla^2\varphi = -qn/\epsilon_0, \tag{3}$$

where field strength B is assumed constant and the boundary condition $\varphi(R_{\text{wall}},\theta,t)=0$, R_{wall}, being the radius of the free-slip boundary, $q=-e$ and ϵ_0 are electronic charge and permitivity of free space, respectively. Consequently, measuring the density of the electron cloud at a point is equivalent to measuring the ''vorticity'' Ω of a Euler fluid $\Omega=\nabla\times\mathbf{v}\cdot\hat{z}=-qn/(\epsilon_0 B)$, similarly ''stream function'' $\psi\equiv\varphi/B$ and $\varphi(R_{\text{wall}},\theta,t)=0$ correspond to ideal, free-slip boundary conditions. Equations (1)–(3) conserve total energy W and total (canonical) angular momentum L defined by

$$W = \frac{1}{2}\int_{r=0}^{r=R_{\text{wall}}}\int_{\theta=0}^{2\pi} qn(r,\theta)\varphi(r,\theta)r\,dr\,d\theta \tag{4}$$

and

$$L = \frac{qB}{2}\int_{r=0}^{r=R_{\text{wall}}}\int_{\theta=0}^{2\pi} n(r,\theta)r^2\,r\,dr\,d\theta, \tag{5}$$

respectively. Conservation of W and L is a consequence of stationarity and symmetry of the confining boundary, respectively. Furthermore, any integral of a regular function of density n (or vorticity Ω) over the domain is also a constant of motion; consequently, the set of functions $\{C_j\}$ defined by

$$C_j = \int_{r=0}^{r=R_{\text{wall}}}\int_{\theta=0}^{2\pi} n^j(r,\theta)\,r\,dr\,d\theta, \quad j=0,1,2,...,\infty \tag{6}$$

represent an infinite set of invariants (sometimes called Casimir invariants), which follows from conservation of density (vorticity) along the flow trajectories, Eq. (1). Out of the conserved quantities defined by Eqs. (4)–(6), *robust* invariants are W, L, C_0, and C_1, while higher order Casimir invariants are regarded as *fragile*. Note that C_0 and C_1 merely imply constancy of area (incompressibility) and total charge (circulation), respectively.

Recently, this homology between the 2D drift-Poisson model of strongly magnetized plasmas and the equations governing 2D Euler flows has given rise to a spurt of theoretical,[4–7] experimental,[9–11] and numerical[12] studies related to the dynamics of intense point-like vortices with a background flow. Most previous works[6,7,9–12] have either considered strong intense vortices evolving from unstable initial conditions which eventually give rise to ordered patterns *and* a background or assume that the point-like vortices are already within the background flow. Similarly, studies in

[a]Present address: EPFL, 1015 Lausanne, Switzerland.
[b]Electronic mail: jkl@galaxy.postech.ac.kr

hole dynamics have been restricted in the past to either initial conditions of a hollow electron column[13] wherein these holes are reported to give way to axisymmetric minimum enstrophy vortex states (selective decay) over a few hundred turnover periods or to a single hole/vortex configuration in a nonuniform shear flow.[14]

Studies pertaining to the equilibrium and dynamics of isolated vortex patches in an unbounded domain have also been extensive. For example, it is well known that circular uniform vortices in an otherwise unbounded, irrotational flow, called ''Rankine vortices'' support surface waves (also called ''Kelvin waves'') on its boundary. These waves are in general known to be marginally stable (i.e., Im $\omega \equiv 0$). Deem and Zabusky[15] numerically showed the existence of a ''continuum'' of Kelvin waves with m-fold symmetry called ''V-states'' which are *nonlinear dispersive* modes with angular velocity less than that of *linear* Kelvin waves. These authors noted that V-states play a crucial role in the onset of ''filamentation'' process (thin filaments of vorticity drawn off the patch). The late time filamentation of an *infinitesimally* small perturbation to a Rankine vortex was studied in detail by Dritschel[16] (though Pullin[17] had earlier suggested the possibility); these works were later supported by Pullin and Moore[18] and Polvani *et al.*[19] who studied the filamentation onset time for a *unstable harmonic* perturbation to the Rankine vortex. More recently, the fact that the Kelvin waves are *negative energy* waves, whereas the interaction energy between a point-like vortex and a *nearly* circular patch is *positive*, was exploited by Lansky *et al.*[4] in their resonance cascade model of merger of asymmetric vortices in unbounded domain. In yet another study, Jin *et al.*[7] have considered a collection of point-like intense vortices placed *inside* a Rankine vortex. They show the existence of *fast* and *slow* time filamentation, the former originating due to the interaction of Kelvin waves and the latter due to the interaction of point-like vortices and the Rankine vortex. These studies are based on either theory and/or Contour Dynamics (CD) simulations.[20] Unfortunately, analytical methods to study beyond wave breaking (let alone mixing and merger) are marred by difficulties, whereas CD methods are known to fail with the onset of ''wave overturning'' or wave breaking.

A collection of point-like vortices arranged in a ring(s), their equilibrium and stability have also been extensively studied in the past. For example, Havelock[21] showed that, for an unbounded system, if N_{pv} (number of point-like vortices arranged in a ring configuration) is such that $N_{pv}<7$, the configuration is stable, whereas for $N_{pv}>7$, it is unstable; similarly for simply bounded domains $N_{pv}\leqslant 6$ is stable and $N_{pv}\geqslant 7$ is unstable; later Campbell[22] studied, using theory and extensive simulations, such ordered point-like vortex patterns both without and with a boundary; more recently Lansky *et al.*[5] have worked out the stability analysis of N_{pv} point-like vortices in a ring with a central point-like vortex of arbitrary strength, all enclosed within a circular, free-slip boundary. Experiments on a collection of point-like vortices within a background vortex flow using single species electron plasmas have also been performed.[10,11]

In the present work, we focus on a model wherein a collection of *ordered* intense, point-like vortices is placed initially *outside* of a uniform circular patch, and both point-like vortices and patch are enclosed within a circular, free-slip boundary. This system is then numerically time evolved for about 10–15 patch turn over times (defined below). Motivation for studying this particular model is to understand whether a *prearranged* N_{pv} number of point-like intense vortices sustain its symmetry through the merger process and finally form ''patterns'' within the patch vortex which may then be regarded as a ''well mixed background flow.'' In our simulations, the dynamics of point-like vortex with patch is shown to proceed by (i) formation of quasistationary bounded V-states,[15] (ii) filamentation and wavebreaking; (iii) hole capture and transient hole patterns generated within the patch leading finally to (iv) sustained vortex patterns and a background flow. The relative strength of a point-like vortex normalized to that of the patch, Γ, defined as

$$\Gamma = \sum_{i=1}^{N_{pv}} \frac{\Gamma_i(pv)/N_{pv}}{\Gamma_{pa}}$$

[where $\Gamma_i(pv)$ is the strength of individual point-like vortices and Γ_{pa} is the strength of the patch] is moderate ($1.0\times 10^{-2}<\Gamma<1.0\times 10^{-1}$). We first present our simulational tool in Sec. II. In Sec. III, we present some relevant physics issues and point out certain specific features of our choice of initial condition. In Sec. IV, starting from this initial condition, we demonstrate that the pattern sustains itself finally leading to self-consistent vortex–hole patterns followed by hole-dynamics and stabilization of vortex patterns at a particular final radial position. A simple physical model based on conservation of robust invariants is presented. Novel results at each stage of the evolution are presented in the later sections: (a) the bounded V-states for different values of $\alpha = R_{pa}(\tau=0)/R_{\text{wall}}$ [where $R_{pa}(\tau=0)$ is initial radius of the vortex patch] (Sec. V), (b) *induced* filamentation and wave breaking time t_{wb} is shown to follow a new scaling law (Sec. VI). In Sec. VII, we present some conclusions.

II. SIMULATIONAL TOOL: A PARTICLE-IN-CELL CODE

We begin by first discussing the numerical issues. We use an electrostatic particle-in-cell (PIC) code XPDC2 (Refs. 23, 24) which for the present work, solves 2D drift-Poisson equations [Eqs. (1)–(3) above] on a uniform grid in the $r-\theta$ plane. The length of the cylinder along the $\hat{z}$-direction is assumed large compared to the radius of the circular vessel. Thus the dynamics is restricted to the $r-\theta$ plane.

The basic idea is to exploit the fact that a ''point vortex'' is a *weak* solution to the drift-Poisson (Euler) equation with the consequence that a given initial distribution of density (vorticity) may be well approximated by sufficiently large number of such point vortices. This discretization procedure allows the equations of motion to be cast in (noncanonical) Hamiltonian form with the coordinate space itself being the *phase space*. In principle, one may use standard methods (such as Symplectic integration) of dynamical systems theory for further evolution. As said before, in order to closely approximate the ''continuum'' distribution of interest, it becomes necessary to use large number of simulational particles N_s (i.e., 2 N_s degree of freedom). Consequently, in

the present work, we use the standard PIC method. [Since the ''particles'' are point vortices, this method, as applied to such systems is, sometimes referred to as the vortex-in-cell (VIC) method.] Thus, the ''particles'' (point-vortices) in *phase space* $[r-\theta]$ are coarse grained by superposing a uniform grid in $r-\theta$. Density is obtained by interpolating (area-weighting)[24] from the point-vortices to a uniform grid (typically 100×256) on which Poisson's equation is solved by fast Fourier transformation in θ and 3-point finite difference scheme in r directions, respectively, with free-slip boundary at R_{wall}. The electric (velocity) field is obtained on the grid points which is interpolated back to the ''particle'' positions. Integrations in time are fully second-order accurate.

Note that, at any given time, the locations of the simulational particles, represent a *complete N-body* description, while density (vorticity) distribution may be regarded as ''coarse-grained.'' Thus, experimentally measured electron density (vorticity) pertains to the coarse-grained quantities. However, to elucidate certain fine-scale features of filamentation and axisymmetrization, some of our results are presented as *phase space* profiles and coarse-grained profiles as and when necessary. To benchmark the code we have performed a number of tests viz., (i) when loaded with a circular uniform density electron cloud at the center of the system (Rankine vortex), a ''fluid particle'' on the circumference of the patch completes one rotation in exactly one patch turnover time (defined below); (ii) when loaded with a Rankine vortex plus a linear perturbation, the resultant surface waves (Kelvin waves) are found to be marginally stable. The surface waves are observed to persist without growth or decay for as long as the numerical dissipation is small; (iii) hollow electron cloud of uniform density (annular vortex patch) plus a perturbation exhibits linear diocotron (or Kelvin–Helmholtz) instability. In the worst cases, the growth rate agrees with the theoretical values[3] to within a factor of 2. (iv) A number of point-like vortices N_{pv} (Havelock patterns) without the uniform background vorticity, arranged in rings of normalized radius R_{pv}/R_{wall} (without a central point-like vortex) were loaded. For $N_{pv}<7$, the code reproduces the well-known Havelock stability bounds on R_{pv}/R_{wall} (Ref. 22). To illustrate the results, in Fig. 1, for $R_{pv}/R_{\text{wall}}=0.25$, the pattern lifetimes for various numbers of point-like vortices N_{pv} is shown. Here, time is normalized to $t_D=3.47\times10^{-3}$ s, which would correspond to the turnover time of a patch of density $n_{pa}=2\times10^{11}\ \text{m}^{-3}$. Note that at $N_{pv}=7$ there is a sharp transition which is in qualitative agreement with the theory and experiments. There are some differences too. For example, we find that $N_{pv}=7$ is quite unstable, which is rather consistent with the theory but in disagreement with experiments.[11] (v) Finally, as reported elsewhere[23] using a patch and a point-like vortex such that Γ is small $(\approx10^{-3}-1\times10^{-2})$, the code reproduces the resonant cascade merger process.[4] However, due to the presence of the circular conducting wall, the resonance surfaces are shifted *inwards* and the magnitude of Γ_c as well as the merger spectrum (Fig. 4 of Ref. 4) appear altered. Also, a novel phenomenon of a point-like vortex acting as a ''mixing agent'' is demonstrated numerically in the large Γ limit.[23] Furthermore,

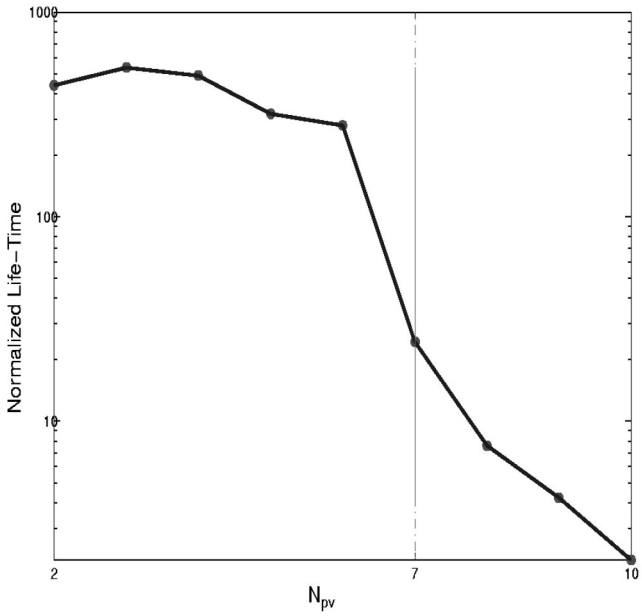

FIG. 1. For $N_{pv}=2-10$, the Havelock stability is numerically tested for $R_{pv}/R_{\text{wall}}=0.25$ which is below the critical radii for instability. Good qualitative and reasonable quantitative agreement is seen. For this run, $n_{pv}=1\times10^{13}\ \text{m}^{-3}$ and $B=1$ T. For comparison, time is normalized to $t_D=3.47\times10^{-3}$ s which corresponds to a turnover time of a uniform patch with density $n_{\text{pa}}=2\times10^{11}\ \text{m}^{-3}$.

robust integral invariants, such as total charge (circulation), total electrostatic energy (flow kinetic energy), and total angular momentum (total angular impulse), are conserved to within 2% of their initial values for a decade or more of diocotron (vortex turn over) period. The results appear not to change with variation in the number of simulation particles N_s (typically, $N_s\approx2\times10^4-8\times10^4$) or by changing the grid size (100×256) by a factor 2 or more. However, at much later times $(\geqslant50\tau_D)$ we observe numerical central density fluctuations at $r=0$ ($\leqslant5\%$ of the mean) arising due to uniform gridding in $r-\theta$, which we consider as a nonissue for the present purposes $(t\leqslant15\tau_D)$.

For all the data presented below, the following parameters are used unless stated otherwise. Axial magnetic field $B=1.0$ T, length of the circular cylinder $L_z=1.0$ m, radius of the circular conducting wall $R_{\text{wall}}=2\times10^{-2}$ m, radius and density of the vortex patch $R_{\text{pa}}=6.0\times10^{-3}$ m and $n_{\text{pa}}=1.8\times10^{12}\ \text{m}^{-3}$, the vortex patch turnover time $t_D=2\pi/\omega_E\simeq3.86\times10^{-4}$ s (ω_E is the diocotron frequency of the patch), initial (peak) density of point-like vortices $n_{pv}=1\times10^{13}\ \text{m}^{-3}$ and initial radial location $R_{pv}\simeq8\times10^{-3}$ m. Note that $R_{pv}/R_{\text{wall}}=0.4$ is much below the minimum critical radius for Havelock instability for $N_{pv}<7$. Thus, without the vortex patch, the point-like intense vortex patterns on a ring are stable configurations and the merger is only due to the interaction of the point-like vortices with the patch. Above said parameters are so chosen that the results reported here may be tested in a laboratory. All results are presented in laboratory frame of reference.

In the next sections to follow, we will first highlight some important physics issues of interest, then give a dynamical picture starting from initial condition until the vor-

tex pattern stabilizes well after the hole pattern is sheared out by the diocotron instability. In the later sections, a detailed analysis at each stage of the evolution is presented.

III. PHYSICS ISSUES

As pointed out in the Introduction, the basic idea in the present work is to show in a simple way, an alternate method to form patterns which have been observed in 2D electron fluid experiments. Here, we have used a novel initial condition of many point-like vortices (whose strength is extracted from final states of vortex pattern experiments of Fine *et al.*[9]) arranged on a ring, with N_{pv}-fold symmetry in θ-direction. This pattern interacts with a uniform density vortex patch by exciting surface wave with mode number $m=N_{pv}$.

Unlike the previous works,[5,7] where either a *resonant cascade model*[5] or a collective excitation of many surface waves[7] is used, in the present model, the only dominant mode is $m=N_{pv}$. This particular surface wave is driven (by extracting energy from it) to its maximum amplitude to form an equivalent of a ''*V*-state'' [15] in a bounded domain. This N_{pv}-polygon vortex patch would now have N_{pv} vertices with a 90° intercepted between its sides at each vertex. The proximity of the point-like vortices (which by now, may or may not have actually merged with the patch) to the vertices of the bounded *V*-state, induces a filamentation process (pinching off very fine filaments of vorticity).[16] These filaments then encircle the point-like vortex patterns in the shear flow created by the vortex patch generating vortex–hole patterns. This hole pattern would then become (Kelvin–Helmholtz or Diocotron) unstable stirring up the patch and finally the vortex pattern stabilize. In general, depending on the choice of the initial radial location of the point-like vortex pattern and/or the relative strength Γ, the above described nonlinear merger process may be interrupted. For example, if the initial radial location is far away so that the induced filamentation process of the vertex (edge of the *V*-state) is weak or if the relative strength of the point-like vortices is such that the patch is unable to form a bounded *V*-state, then the above said process may fail to effect a merger and thus one may be left with quasistationary locked modes (Havelock patterns)[5,21,22] of point-like vortices and a central extended patch. However, in the present work, the value of relative strength Γ has been set close to that of the patterns obtained in experiments of Fine *et al.*[8,9] Similarly, the initial radial location is set close to the last resonant surface (i.e., $m=2$) for convenience. In the next section, we demonstrate the above said process, numerically, for the case $N_{pv}=5$.

IV. PATTERN SUSTENANCE: A DYNAMICAL PICTURE

We discuss below the case of $N_{pv}=5$ point-like vortices initialized at a given radial location but equispaced in θ outside the patch [Fig. 2(a)], as a prototype for which the bounded *V*-states, filamentation, wave-breaking, and hole capture occurs in typically about 2.6 turnover periods. The conservation of robust invariants, such as total energy and total angular momentum, for this case is shown in Fig. 2(b). By construction, our code conserves C_0 and C_1, whereas the higher order Casimir C_j, $j\geqslant 2$ are found to be violated in the coarse-grained sense. The physical process described below for $N_{pv}=5$ is found to be generic and similar process is seen for all other N_{pv} $(2\leqslant N_{pv}\leqslant 10)$ values.

The point-like vortices become unstable due to the presence of the central Rankine vortex. As they fall toward the boundary of the patch, a surface wave of mode number N_{pv} is excited. The amplitude constantly grows as the distance between the point-like vortices and the patch decreases. The N_{pv}-surface mode transforms from a linear Kelvin wave into a nonlinear mode (*V*-state). As noted by Deem and Zabusky,[15] these *V*-states are generalizations of Kelvin waves with N_{pv}-polygonal symmetry, but with a notable difference; due to the presence of the conducting wall at $r=R_{\text{wall}}$ (a free-slip boundary), the period of rotation is now significantly altered. A comparison with the unbounded *V*-states studied by Deem *et al.* and the effect of variation of patch size in bounded domain (i.e., variation of α) is presented in the upcoming sections.

As the point-like vortices continue to fall, they drive the N_{pv}-polygons to their state of maximum curvature[26] at the corners. When the corners become cusp-like,[26] the point-like vortices draw off fingers from the infinite curvature points of the patch in about $\tau=t/t_D\simeq 0.62$. These fingers then grow further in their amplitude until ''purely radial'' structures are developed, whereafter, these fingers ''wave break'' under the shear flow generated by the patch plus point-like vortices and convert themselves into θ dependent structures thus enveloping the point-like vortices (see Fig. 3). While the unstable point-like vortices are drawn further into the patch, the fingers grow and tend to symmetrize about the patch in the shear generated by the patch [Fig. 2(a), second row]. This process traps symmetric ''hole'' regions into the ''born-again'' patch vortex ($\tau\simeq 3$).

These symmetric ''vortex–hole'' pattern sustains itself for another two turnover periods (until $\tau\simeq 5$) at that time the ''hole'' structures are sheared by the flow and the diocotron instability leads to further ''mixing'' of the patch. Note that the radial location of the vortex pattern oscillates. This is because the point vortices are coupled to their hole counterparts through angular momentum conservation [see Fig. 2(b)]. Consequently, the radius of the point-like vortex patterns does not stabilize until after nearly all the holes are sheared and ''filled-in.'' This happens at about $\tau\simeq 6.4$ [see last row, Fig. 2(a)]. The radial position of the point-like vortex pattern, $R_{pv}(\tau)$, reaches a self-consistent, nearly constant value at about $\tau=6.4$, whereafter the radius of the vortex pattern does not alter significantly. The size of the vortex patch expands to 1.5 times its initial radius. The radius of the pattern normalized to initial patch radius, $R_{pv}(\tau>6.5)/R_{pa}(\tau=0)\simeq 0.54$. The simulation is carried on to about $\tau=13$ without any significant change in the radial location of the vortex pattern.

It is interesting to note that during merger, the point-like intense vortex [see Fig. 3(d)] is subject to large shear forces by the patch. Consequently, the point-like vortex develops a central ''core'' and a ''diffused'' halo around the core, which may eventually get smeared away, depending on the value of Γ.

In Figs. 4(a) and 4(b), the states at hole capture time

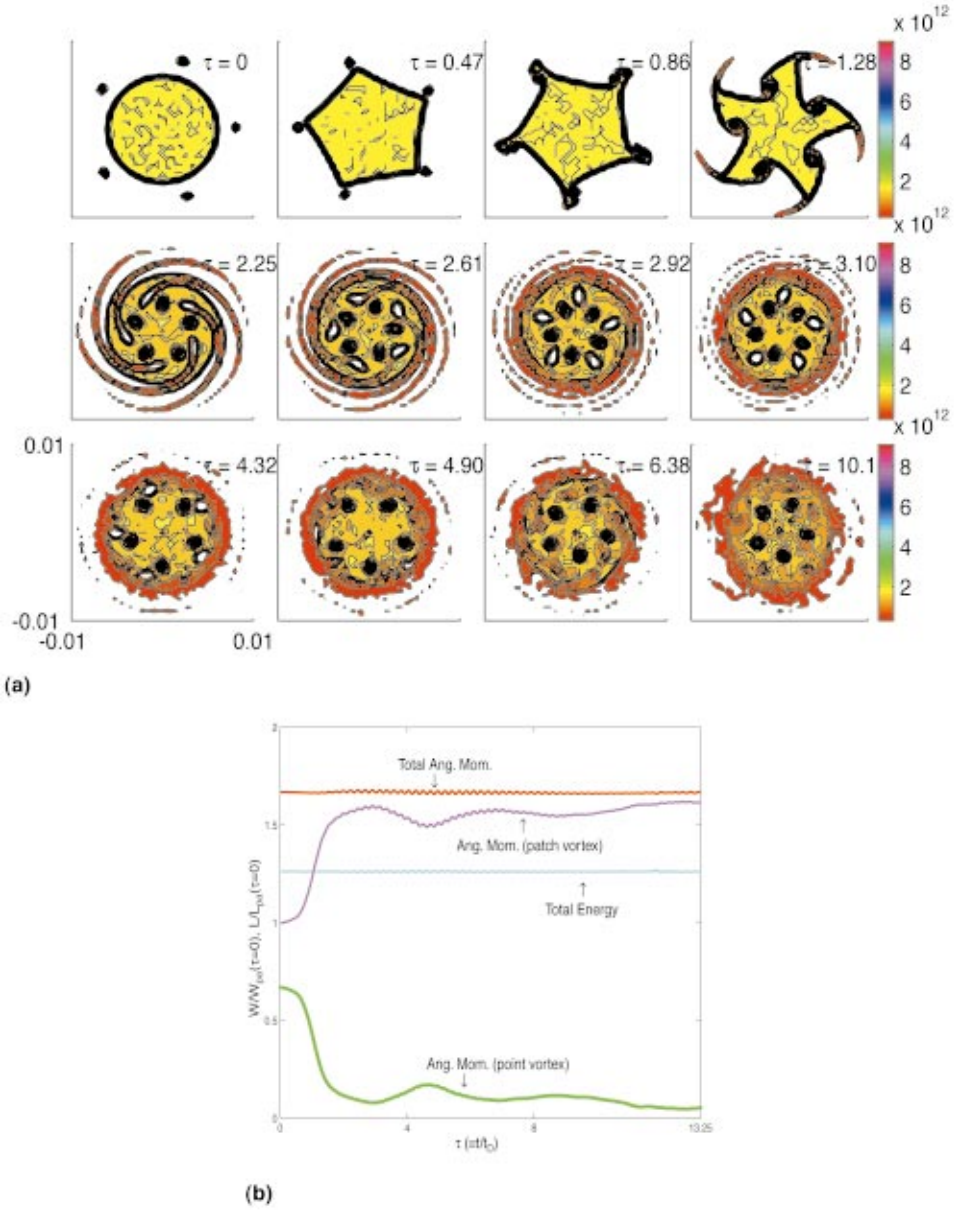

FIG. 2. (a) (Color) The density (vorticity) contour plot for $N_{pv}=5$, the process of the bounded V-state, filamentation and wavebreaking, vortex capture by shear, formation of hole pattern, and the late stage vortex patterns are shown in the *lab*-frame. For this run $\Gamma \simeq 3.7\times10^{-2}$. For presentation purposes, the outer wall at $R_{\text{wall}}=2\times10^{-2}$ m is not shown. The horizontal axis is $\hat{x}$ and the vertical axis is $\hat{y}$. (b) Conservation of total energy W [Eq. (4)] and total angular momentum L normalized to the initial energy $W_{\text{pa}}(\tau=0)=1.401\,78\times10^{-11}$ J and initial angular momentum $L_{\text{pa}}(\tau=0)=-2.935\,147\times10^{-16}$ J s of the patch.

(column 1), the state before the hole pattern is sheared apart (column 2) and a late time state (column 3) [where, for some cases, only point-like vortices exist] are shown for $N_{pv}=2$, 3, 4, 6, 7, 8, 9, and 10 [for $N_{pv}=5$, see Fig. 2(a)]. For the same radial locations, we find that for given value of N_{pv}, the area of hole captured increases with the strength Γ. This is because, to conserve L, the amplitude of the purely radial fingers before wavebreaking scales with Γ. Also for a given value of N_{pv}, sustenance of a vortex pattern scales inversely with the area of the hole captured, which in turn depends on the initial radial location of the point vortices (hence the total angular momentum) and the strength of the point vortices. For example, where the hole capture is weak [see Fig. 2(a), column 3], the point vortices sustain the pattern (for as long as the simulations are valid), whereas, the relaxation of larger holes into ''filled-up'' areas destabilizes the vortex pattern. Thus, the size of the hole captured determines the eventual stability of the vortex patterns. Furthermore, as shown in Fig. 4(b), it may be of interest to note that while the lifetime of Havelock patterns for $N_{pv}>7$ are only a few turnover periods, the ''hole-packed'' patterns inside the patch sustain their discrete θ-symmetry for longer periods. However, as demonstrated in experiments[10] and other studies,[22] for $N_{pv}\geqslant 7$, patterns inside the patch necessarily rearrange, merge, and finally evolve into patterns which may or may not retain their initial symmetry.

Patterns observed in our simulations may have a direct relevance to those observed in recent vortex ''crystal'' experiments.[6,9,11,12] As shown by the experiments,[10,11] once intense point-like vortices with a symmetry are assumed in a background, they are shown to be sustained. Also, a random arrangement of point-like vortices in a background are found to ''crystallize.'' The novelty of our simulations is that from an initially unstable *symmetric* patterns, the point-like vortices are self-consistently shown to merge via formation of bounded V-states, induced filamentation and wavebreaking,

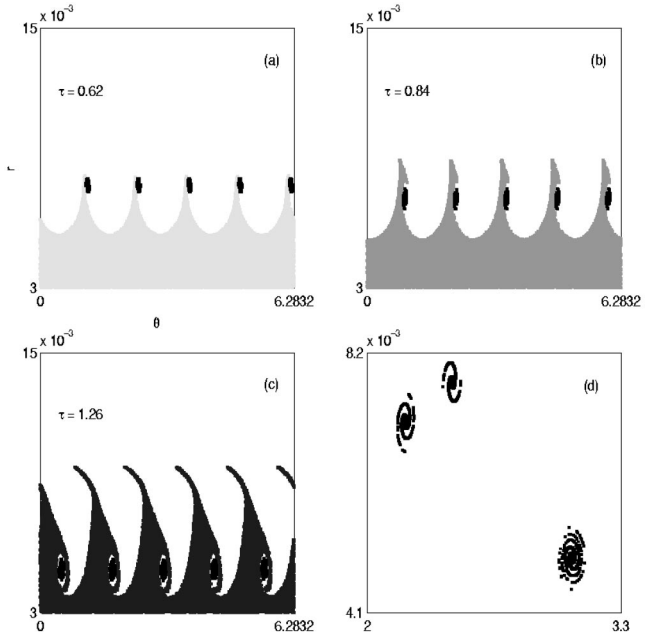

FIG. 3. Wavebreaking of the patch (surface) and structure of the point-like intense vortex during merger from $N_{pv}=5$ datum. In (d), the structure of a point-like vortex at three different times corresponding to (a), (b), and (c) is presented. The plots are shown in *phase space* (r, θ).

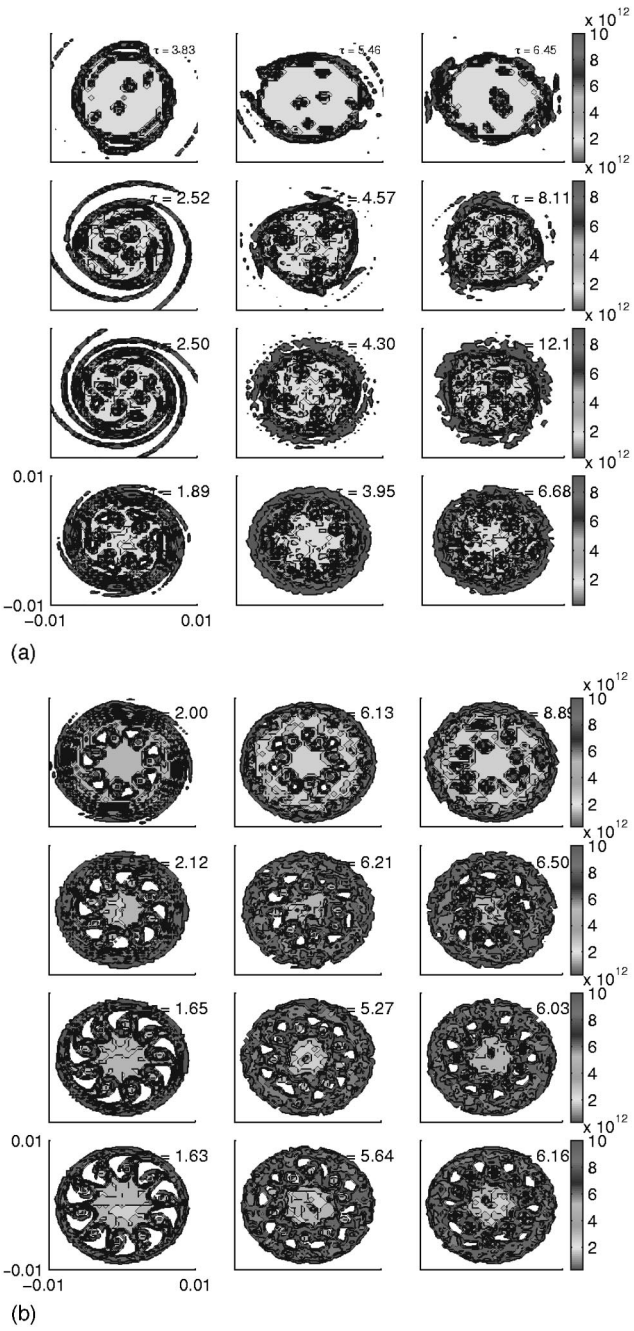

FIG. 4. (a) Density (vorticity) contour plots for $N_{pv}=2$, 3, 4, and 6, the captured hole (first column) state, hole shear state (second column), and vortex patterns at late times (third column) are shown in the *lab*-frame. The horizontal axis is $\hat{x}$ and the vertical axis is $\hat{y}$. (b) Details same as above for $N_{pv}=7$, 8, 9, 10. Except for the $N_{pv}=7$ case, the ''hole-packed'' vortex patterns inside the patch are sustained for a relatively longer time than the Havelock pattern (Fig. 1).

hole capture, relaxation, and attain quasisteady state with a stirred up background.

Furthermore, it is interesting to note that the regional maximum entropy theory,[6] which presupposes N_{pv} number of strong point vortices and extremizes the entropy of the background flow, seem to predict the location R_{pv} accurately. As discussed before, our vortex-hole patterns first ''mix up'' the patch (i.e., the background flow) and the flow in turn appears to ''stabilize'' the pattern. Though we have not accurately estimated the level of background stir-up (for example, a correlation function study of a passive scalar in the background), the near-constant values of $R_{pv}(N_{pv}=5)$ after $\tau=6.4$ suggests that the patch (background) is well mixed. Also, the reported time for crystal formation is typically about 10 turnover periods,[9,11,12] our ''equilibration'' or ''hole disappearance time'' for most cases of N_{pv} is about 6–8 turnover periods. Furthermore, it is known from experiments that certain striated initial conditions[12] (for example, nonuniform spiral density case) are known to ''seed'' the crystallization process. Yet, there is no clear understanding of why these initial conditions give rise to crystal patterns, whereas other *similar* initial conditions do not. Also certain angular momentum constraints are understood to provide bounds for crystallization.

Our simulations could provide a novel way to answer these questions. For example, since the point-like intense vortices carry substantial portion of the total angular momentum [see Fig. 2(b)] and could be regarded as the ''striated'' portion of the ''spiral'' while the rest of the ''spiral'' which eventually forms the background vorticity could be the patch which ''equilibrates'' with our vortex patterns. Preliminary results obtained by changing the radial position and relative strength Γ of the point-like vortices are encouraging. This work will be reported in a future communication. Also, it would be interesting to study a Moore–Saffman-type model[26] for relatively long-lived hole patterns (for example, for large N_{pv}) considering them as ''equilibria.''

V. BOUNDED *V*-STATES

Since surface waves are negative energy waves, the point-like vortices gain the necessary energy required to

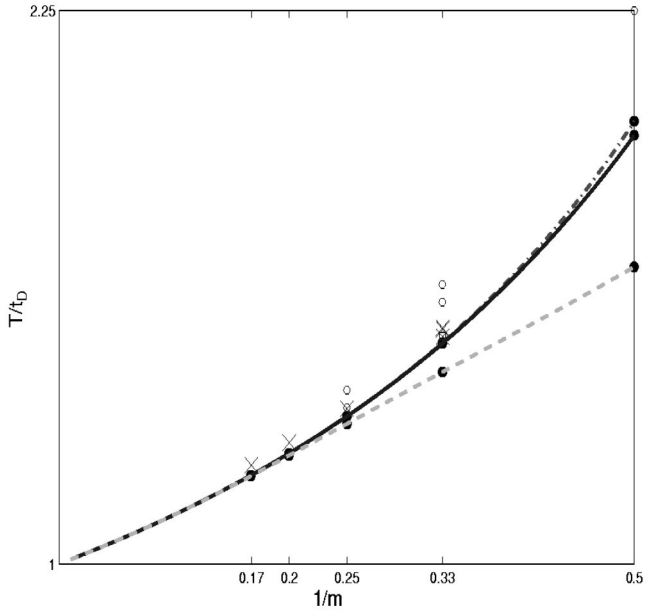

FIG. 5. Equation (8) is plotted with $1/m$ on the x-axis and T/t_D on the y-axis. The dotted–dashed line is for $\alpha=0$ (unbounded case). The solid line is for $\alpha=0.3$ and the dashed line is for $\alpha=0.56$. The points mark the V-states. Open circles (○) are the results of Ref. 15, crosses (×) and squares are for $\alpha=0.3$ and $\alpha=0.56$ bounded V-states.

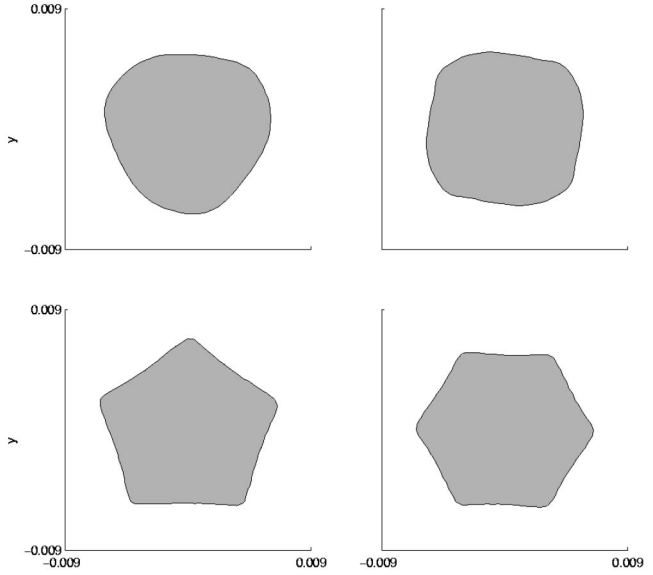

FIG. 6. Numerically obtained shapes of bounded V-states corresponding to the points shown in Fig. 5 for $m=3$, 4, 5, and 6; $V_B(0.3,3,1.53)$, $V_B(0.3,4,1.35)$, $V_B(0.3,5,1.27)$, $V_B(0.3,6,1.22)$. For steady state, viewing in an appropriate frame of reference rotating with period(s) given is necessary.

come close to the boundary by exciting the surface waves whose amplitude increases as the point-like vortices come close to the boundary. Note that in contrast to the model reported in Ref. 4, where a single point-like vortex placed at a critical radial position with a certain relative strength, either oscillates or excites *higher* order modes resonantly as it ''falls'' toward the patch, here, due to the presence of N_{pv} number of point-like vortices, only a *particular* surface wave of mode number N_{pv} is excited.

To demonstrate the nature of the V-state, we perform the following *Gedanken* numerically: Amplitude of a particular surface wave depends upon how close is the point-like vortex pattern from the patch boundary. Consequently, one may precisely control the amplitude (and hence period of rotation of the V-state) by *removing off* the *inducing* point-like vortices from the simulation domain, when a desired amplitude is reached. This results in a V-state inside a free-slip boundary. Period, shape and other properties thus obtained for $N_{pv}=3$, 4, 5, and 6 are shown in Figs. 5 and 6.

As noted, earlier workers,[15,26] the family of V-states may be regarded as nonlinear modes which form a two-parameter family of angular frequency and amplitude. If the amplitude(s) is infinitesimal, they are the usual *Kelvin waves*. As their amplitude is increased, each branch ($N_{pv}\geqslant 3$) ends in a polygon with sharp corners (cusps) with *infinite curvature* at the corners.

Following Deem *et al.*, we characterize bounded V-states as $V_B(\alpha,N_{pv},T)$, where $\alpha=R_{pa}(\tau=0)/R_{\text{wall}}$ and T is the period of state. Linear dispersion relation for Kelvin waves in a simply connected domain and free-slip boundary is given by

$$\omega_L=\omega_E(m-1+\alpha^{2m}), \tag{7}$$

where ω_E is the Diocotron frequency (defined at the end of Sec. II). Thus the waves have a rotation period of T_L given by

$$T_L=t_D m/(m-1+\alpha^{2m}) \quad \text{and} \quad t_D=2\pi/\omega_E. \tag{8}$$

In Fig. 5, Eq. (8) is plotted for $\alpha=0$, 0.3, 0.56. As can be expected from Eq. (8), the bounded V-states have, in general, smaller periods as compared to their unbounded counterparts. Also, we find that for α-values beyond 0.56, we are unable to initialize a *single* surface mode N_{pv}. Though a order of magnitude lesser, a weak 2 N_{pv} mode always induces itself on the surface for values of α larger than 0.56. For example, for $N_{pv}=3$ and $\alpha>0.56$, irrespective of the initial radial position of the point-like vortex pattern, there is always an accompanying 2 N_{pv} mode (i.e., mode number 6). Thus the V-state is of ''mixed'' kind. Such states quickly (in $<1t_D$) develop kinks on their surface. In Fig. 7, we present bounded V-states $V_B(0.56,3,1.468)$ and $V_B(0.6,3,1.483)$ which shows the onset of ''kink'' phenomenon due to the proximity of the free-slip boundary R_{wall} to the patch boundary. The period for the kink V-state is only formal. At about 0.68 t_D the kink onset begins, which eventually (about 1.52

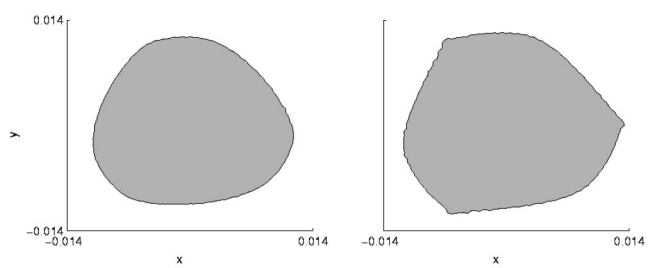

FIG. 7. Bounded V-states showing existence of critical $\alpha\simeq 0.56$ beyond which ''mixed'' V-states exist. On the left is the ''pure V-state'' for $\alpha=0.56$ and on to the right is the ''mixed'' V-state for $\alpha=0.6$. Density is uniform and is shown in false color.

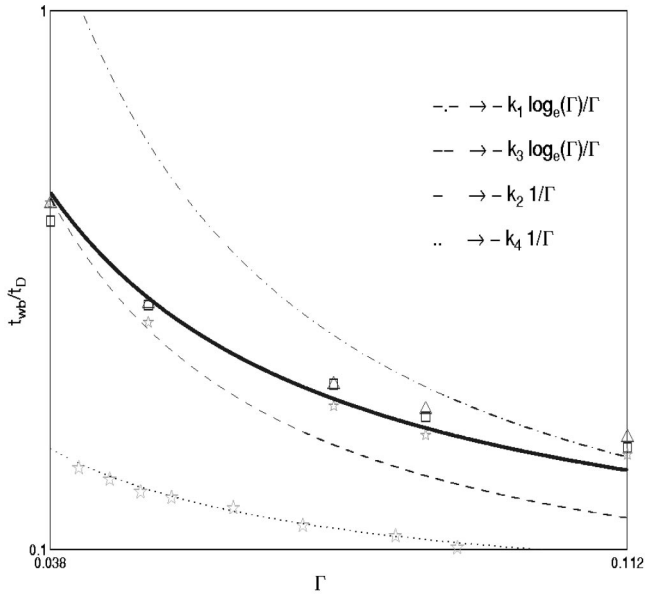

FIG. 8. Γ vs t_{wb}/t_D (the wavebreaking time) for two different values of $R_{pv}(\tau=0)=8\times10^{-3}$ m and $R_{pv}(\tau=0)=7\times10^{-3}$ m is shown. Solid and dotted lines are fit curves [Eq. (9)] for $k=k_2=2.6\times10^{2}$ and $k=k_4=1\times10^{-2}$, respectively. For comparison and visual aid, late-time filamentation scaling from Ref. 7 is shown for two values of the fit parameter $k_1=1.3\times10^{-2}$ and $k_3=7.8\times10^{-3}$. Upper triangles, square, and pentagonal points represent numerically obtained t_{wb} for $R_{pv}(\tau=0)=8.0\times10^{-3}$ m corresponding to $N_{pv}=3$, 4, 5; the lower pentagonal points are for $R_{pv}(\tau=0)=7.0\times10^{-3}$ m for $N_{pv}=5$.

t_D) leads not only to small scale filamentation but to distortion of the patch. As we will see (Sec. VI), the *induced* filamentation in the presence of point-like vortex pattern(s) is faster than *uninduced* filamentation resulting from mixed, bounded *V*-states described above.

VI. FILAMENTATION AND WAVE BREAKING

If the point-like patterns are allowed to further fall continually toward the distorted vortex patch boundary, quickly the patch develops N_{pv} number of cusps with very large curvature. From these cusps emanate thin filaments of vorticity. Filaments grow until they become ''purely radial'' while, the point-like vortex pattern fall further into the patch. Eventually, the radial fingers overturn and wave-break under the shear flow generated by the patch and the point-like vortex patterns. In Fig. 8, onset time for the process of filamentation and wavebreaking t_{wb} is plotted for $N_{pv}=3$, 4, and 5 as a function of the relative point-like vortex strength Γ; t_{wb} scales as

$$\frac{t_{\mathrm{wb}}}{t_D}=-k/\Gamma. \tag{9}$$

Filamentation and development of fine scales in physical models governed by morphologically similar ''collisionless,'' convective, nonlinear equations such as Euler equations in 2D and Vlasov–Maxwell equations in 6D, is a fundamental issue. For 2D Euler flows, Dritschel[16] and Pullin *et al.*[18] first demonstrated that any *infinitesimal* perturbation to a Rankine vortex (or vorticity slab) has tendency to undergo repeated filamentation after long time, despite nonlinear stability bounds proved by Wan and Pulvirenti[25] for radial displacement of a Rankine vortex boundary. As argued by Dritschel, these bounds do not restrict *local*, detailed vorticity changes; for example, they do not restrict growth in the vorticity gradients ($\nabla\Omega$) but only sets an upper limit on the bulk radial displacement of vorticity.

If $\tilde{R}$ is the radius of the Rankine vortex, $\tilde{l}$, $\tilde{h}$ are the width and height of the perturbation to the vortex respectively, then the filamentation studied by Dritschel[16,26] scales as

$$\frac{t_{\mathrm{wb}}^{\mathrm{Dritschel}}}{t_D}=\frac{\tilde{l}^2}{8\pi^2\tilde{h}^2}\left(15+\frac{100\tilde{l}}{\pi\tilde{R}}\right). \tag{10}$$

Clearly, the late-time filamentation process studied by Dritschel and Pullin *et al.* is for generically different situation. Basic differences are (i) a Rankine vortex plus an infinitesimal perturbation (defined by $\tilde{h}$, $\tilde{l}$, above) is shown to exhibit repeated filamentation over *late-times*. For example, if applied to the $N_{pv}=4$ *V*-state (shown in Sec. V) with parameters $\tilde{h}\simeq7\times10^{-4}$ m, $\tilde{l}=4.0\times10^{-3}$ m, and $\tilde{R}\simeq5.8\times10^{-3}$ m, then from Eq. (10), we get $t_{\mathrm{wb}}^{\mathrm{Dritschel}}/t_D\simeq15.28$. From Fig. 8, it is seen that we obtain a scaling 10 times or more faster. (ii) Filamentation process is an *undriven initial value problem* in the case of Dritschel, whereas, in the present case, the point-vortices are continually driving the patch boundary, (iii) the boundary conditions are free-slip here, whereas unbounded case is studied in Ref. 16.

More recently, Jin and Dubin[7] obtained a scaling law for filamentation of the Rankine vortex boundary for the case of N_{pv} point-like vortices initially placed *inside* the vortex patch. These authors report two regimes for filamentation of the vortex boundary (i) when the point-like vortices are very close to the boundary and (ii) when they are far away; in the former case, a fast filamentation ($\simeq 1\, t_D$), due to the *free-streaming* Kelvin waves is obtained while for the latter case, a slow-time filamentation which scales as $t_{\mathrm{wb}}\propto-\ln(\Gamma)/\Gamma$ is obtained.

There are many fundamental differences between the present model and the one reported in Ref. 7. First, characteristics of filamentation and wave-breaking is altered due to the difference in the initial condition and free-slip boundary. Second, due to the presence of N_{pv} of point vortices placed external to the patch, only a single surface is initially excited. Third, after the initial onset of ''kink'' like structures, which are *extrusive*, the filamentation is induced by the *incoming* point-like vortices, as a result, while ''purely radial'' fingers are being drawn out, the proximity of the evolving radial finger to the point-like vortices increases. Finally, from the scaling law shown for two different values of $R_{pv}(\tau=0)$ (in Fig. 8), it is clear that the present model exhibits filamentation and wave-breaking, in a time less than $1\, t_D$. Though, inapplicable, for visual aid, two fit-curves of the slow-time filamentation is also shown in Fig. 8.

VII. CONCLUSION

We have demonstrated numerically that an initially θ-symmetric, prearranged number of point-like vortices become radially unstable due to a Rankine vortex in a free-slip boundary, merge and finally form quasistationary patterns. The initially unstable patterns ''fall'' continually toward the patch vortex boundary, gaining energy from the surface wave and thus exciting nonlinear, bounded, dispersive modes (bounded V-states), followed by filamentation at the cusps, wave-breaking and vortex–hole capture due to the combined shear of patch and point-like vortices. Conservation of angular momentum dictates further evolution of hole and vortex patterns. Depending upon the angular momentum value, the patterns may sustain inside the patch and form a steady state. Other new results include, demonstration of bounded V-states and a new scaling law for filamentation and wave-breaking.

As discussed in Sec. III, our choice of parameters of initial condition is very specific. A more detailed study of variation of initial position of the point-like vortex patterns and the relative strengths will be reported elsewhere. Finally, for initial conditions as ours, but which break the discrete θ symmetry, merger, hole dynamics and the late-time state of point-like vortices remains to be explored.

ACKNOWLEDGMENTS

One of the authors (R.G.) would like to thank Dr. H. J. Lee for his initial help with the code.

This work was supported by the Korea Research Foundation Grant No. KRF-2000-015-DS0010.

[1] P. Tabeling, S. Burkhart, O. Cardoso, and H. Willaime, Phys. Rev. Lett. **67**, 3772 (1991).
[2] J. C. McWilliams, J. Fluid Mech. **219**, 361 (1990).
[3] R. C. Davidson, *Physics of Nonneutral Plasmas* (Addison–Wesley, California, 1990), pp. 297–304.
[4] I. M. Lansky, T. M. O'Neil, and D. A. Schecter, Phys. Rev. Lett. **79**, 1479 (1997).
[5] I. M. Lansky and T. M. O'Neil, Phys. Rev. E **55**, 7010 (1997).
[6] D. Z. Jin and D. H. E. Dubin, Phys. Rev. Lett. **80**, 4434 (1998).
[7] D. Z. Jin and D. H. E. Dubin, Phys. Fluids **13**, 677 (2001).
[8] D. Z. Jin and D. H. E. Dubin, Phys. Rev. Lett. **84**, 1443 (2000).
[9] K. S. Fine, A. C. Cass, W. G. Flynn, and C. F. Driscoll, Phys. Rev. Lett. **75**, 3277 (1995).
[10] D. Durkin and J. Fajans, Phys. Fluids **12**, 289 (2000).
[11] D. Durkin and J. Fajans, Phys. Rev. Lett. **85**, 4052 (2000).
[12] D. A. Schecter, D. H. E. Dubin, K. S. Fine, and C. F. Driscoll, Phys. Fluids **11**, 905 (1999).
[13] X.-P. Huang, K. S. Fine, and C. F. Driscoll, Phys. Rev. Lett. **74**, 4424 (1995).
[14] D. A. Schecter and D. H. E. Dubin, Phys. Fluids **13**, 1704 (2001).
[15] G. S. Deem and N. J. Zabusky, Phys. Rev. Lett. **40**, 859 (1978).
[16] D. Dritschel, J. Fluid Mech. **194**, 511 (1988).
[17] D. I. Pullin, J. Fluid Mech. **108**, 401 (1981).
[18] D. I. Pullin and D. W. Moore, Phys. Fluids A **2**, 1039 (1990).
[19] L. M. Polvani, G. R. Flierl, and N. J. Zabusky, Phys. Fluids A **1**, 181 (1989).
[20] N. J. Zabusky, M. H. Hughes, and K. V. Roberts, J. Comput. Phys. **30**, 96 (1979).
[21] T. H. Havelock, Philos. Mag. **11**, 617 (1931).
[22] L. J. Campbell, Phys. Rev. A **24**, 1 (1981), and references therein.
[23] R. Ganesh and J. K. Lee, IEEE Trans. Plasma Sci. **30**, 6 (2002).
[24] C. K. Birdsall and A. B. Langdon, *Plasma Physics via Computer Simulation* (Adam Hilger, New York, 1991).
[25] Y. H. Wan and M. Pulvirenti, Commun. Math. Phys. **99**, 435 (1985).
[26] P. G. Saffman, *Vortex Dynamics* (Cambridge University Press, Cambridge, 1992), pp. 116–119, 171–177.